Imbalance Constrained Crossphase Quadratic OPF for Optimal Integration of EV Chargers and PV Inverters in Meshed and Radial Distribution Systems

Araz Bagherzadeh Karimi, *Student Member, IEEE,* Reza Deihimi Kordkandi, *Student Member, IEEE,* Farrokh Aminifar, *Member, IEEE,* Mohsen Hamzeh, *Member, IEEE,*

***Abstract*—Inverter-Based distributed energy resources, specially Photovoltaic devices (PVs) and electric vehicle charge stations (EVCS) in the sequel of the power-electronics interface, provide unprecedented flexibility to the system, such as the ability to transfer line power across phases. This paper proposes a comprehensive framework for per-phase optimal active, reactive, and cross-phase power flow dispatch of PVs and EVCSs. The optimization problem is targeted to maximize the firm benefit of DSO subject to the operational constraints, including unbalanced situation tolerability of loads. The problem is formulated as a quadratic objective function with linearized constraints to maintain tractability with many per-phase meshed buses and constraints. A new approximate equation of voltage unbalance factor (VUF) is introduced and used alongside existing linearized equations of other constraints. The framework's applicability is validated via the unbalanced multi-phase IEEE 33 bus and IEEE 192 bus systems. The results show that the cross-phase capability of PVs and EVs and VUF consideration can significantly help the system to satisfy the voltage imbalance limits while increasing the maximum profit in both their operational and nonoperational modes.**

***Index Terms*—Distributed Energy Resources, Electric Vehicle Charge Stations, Cross-phase power flow, Power Quality, Voltage Imbalance Factor**

NOMENCLATURE

A. General

OF	Objective function

B. Indexes

ℓ	Index of lines
φ, γ	Index of phases
i,j	Index of buses
s	Index of a slack bus

C. Parameters

$\alpha_{i_{mn}}^{\varphi\gamma}$,$\beta_{i_{mn}}^{\varphi\gamma}$,$\delta_{i_{mn}}^{\varphi\gamma}$	VUF quadratic approximation coefficients
c_1^s, c_2^s, c_3^s	Cost coefficients of the power provided by the upper voltage system in slack bus *s*
$P_{i_{EV}}^{sch}$	Scheduled consumed active power of an EVCS
$P_{i_{ld}}^{\varphi}, Q_{i_{ld}}^{\varphi}$	Active and reactive powers consumed by load
$P_{i_{PV}}^{sun}$	Maximum available active power of a PV
$R_{ij}^{\varphi\gamma}, X_{ij}^{\varphi\gamma}$	Total resistance and reactance of line from bus *i* to bus *j* and phase φ to phase γ
S_{ij}^{max}	Phase to neutral rated apparent power flow of line from bus *i* to bus *j*
$S_i^{inv}{}_{PV}, S_i^{inv}{}_{EV}$	Phase to neutral rated powers of a PV and EV
V_i	Three-phase Voltage phasor vector
V_i^{min}, V_i^{max}	Minimum and maximum permissible voltage in bus *i*
VUF_i^{max}	Maximum permissible VUF in bus *i*
w', w_i, w	Weight factors of objective function

D. Variables

$P_{i_{EV}}^{\varphi}, Q_{i_{EV}}^{\varphi}$	Active and reactive powers injected from EV
$P_{i_{PV}}^{\varphi}, Q_{i_{PV}}^{\varphi}$	Active and reactive powers injected from PV
$P_{ij}^{\varphi\gamma}, Q_{ij}^{\varphi\gamma}, S_{ij}^{\varphi\gamma}$	Active, reactive and apparent power flows of line from bus *i*, phase φ to bus *j* and phase φ to phase γ
$P_{i\ inject}^{\varphi}, Q_{i\ inject}^{\varphi}$	The injected active and reactive powers
$V_i^{\varphi}, \theta_i^{\varphi}$	Voltage magnitude and angle in bus *i* and phase φ
VUF_i	Voltage imbalance factor in bus number *i*
VUF_i^{apr}	Voltage imbalance factor approximation in bus number *i*

E. Sets

ϕ	Set of phases
L	Set of lines
N	Set of buses
S	Set of Slack Buses

F. Operators

$\hat{A}$	Linear approximation of A
$\{A\}^+, \{A\}^-$	Positive and negative sequence of the three phase phasor vector A

I. INTRODUCTION

MINIMIZING the loss and the operational cost of distribution networks is a critical goal for distribution system operators (DSOs). Distribution networks, by nature, are unbalanced in terms of voltages and currents because of having untransposed lines [1] in distribution feeders and integrating single-phase generators and loads with highly probabilistic

behavior. While voltage imbalance mainly impacts the customers' power quality, the current imbalance is one of the leading causes of loss increase in distribution networks. Mitigation of current and voltage imbalance sources is a strict technical requirement and has drawn the attention of researchers for many years. We review the approaches revolving around the voltage and current imbalance compensation in the following.

Based on [2], we can decompose the origins of the imbalance into twofold classes: structural and random. The method focusing on the structural aspect includes network reconfiguration [3]–[7] and phase balancing [8]–[10]. These techniques, however, do not have real-time flexibility and continuous controllability for compensating for the random component of imbalance. Static transfer system (STS) based methods are proposed to compensate for this [11]. This method may impose switching transients and is less flexible than power electronics devices with continuous controllability. Device-based compensation has been broadly investigated in the literature proving they can mitigate the current imbalance [12]–[15]. These techniques were rarely implemented, but their integrations are abruptly on the rise due to the proliferation of Distributed Energy Resources (PVs) and Electrical Vehicle Charge Stations (EVCSs).

Local control strategies for leveraging distributed energy PVs for imbalance compensation have been discussed in [16], [17]. These approaches, as expected, are highly effective, but they still lack utilization of total capability of flexible power electronics resources due to the control with incomplete local information status. In the wake of cyber-physical distribution networks enabled by the vast deployment of communication systems, the operational strategies running over the network model with complete system-wide information turn into an actual practice [18]–[23]. These methods accommodate the controllability of PV resources and seek to minimize the operation cost in the presence of distribution network imbalance. Voltage imbalance is tackled as a subsidiary objective function in the optimization problem.

The methods mentioned in the last paragraph mainly revolve around three-phase or single-phase PVs, but none implement the cross-phase capability for the three-phase inverters in their models. In addition, they are either proposing a non-convex model to compromise the computational performance or a convex model, which is only valid in radial topology. Also, due to the rectangular model requirement for those simplifications, the highly non-linear non-convex VUF equation is ignored. Therefore, in this paper, a novel feasible three-phase optimal power flow that can also include the above motioned overlooked aspects is tailored which includes these main features:

- Introducing a Convex (QP) three-phase optimal power flow that models bus voltages in polar form with magnitudes and angles.
- Using linearized load flow equations and capacity constraints that minimize an objective function, including total cost, and a polynomial data-driven approximation of VUF, which is computationally fast and scalable because of convexity and can also be implemented in heavily meshed three-phase distribution networks.
- Participating in the ever-growing three- and single-phase EV chargers alongside three- and single-phase PVs in optimal power flow operation not only to avoid their possible harmful operation but also to exploit the total capacity of installed devices to reduce cost and improve system conditions.
- Introducing Cross-phase operation in three-phase inverter models that can exploit the unused three-phase inverter capacity in terms of active and reactive power in different operational and non-operational modes to improve system conditions and reduce the cost even more.

Various sub-methods and scenarios are created, tested, and compared in IEEE 33 bus radial and 192 bus heavily meshed test systems. The provided results thoroughly compare the scenarios, sub-methods, Inverter devices, and the two topologies regarding cost, loss, and VUF. The results also create a starting point to address these critical questions for DSOs; 1) How much should an inverter or load owner pay for making the system unbalanced? 2) How much should an inverter owner earn to enable the cross-phase operation?

The remainder of this paper is organized as follows. Section II formulates the proposed optimization problem. The computation implementation is described in III. Section IV shows the parameter tuning, while the results and the corresponding discussion are presented in section V. Finally, conclusive remarks are presented in Section VI.

II. Problem Formulation

The optimization problem is based on an OPF model with a single objective function and multiple physical and operational constraints, including the imbalance limits. The convex form of the OPF model is employed here, and the new constraints are convexified to align with the whole model trait.

A. Power Flow model

Three-phase power balance equations consisting of PV injection, EV interaction, and load consumption are expressed as:

$$\forall i \in N, \varphi \in \phi,$$
$$P^{\varphi}_{i_{inject}} + P^{\varphi}_{i_{PV}} = P^{\varphi}_{i_{ld}} + P^{\varphi}_{i_{EV}} + \sum_{j|(i,j)\in L} \sum_{\gamma|\gamma\in\phi} P^{\phi\gamma}_{ij} \quad (1)$$

$$\forall i \in N, \varphi \in \phi,$$
$$Q^{\varphi}_{i_{inject}} + Q^{\varphi}_{i_{PV}} = Q^{\varphi}_{i_{ld}} + Q^{\varphi}_{i_{EV}} + \sum_{j|(i,j)\in L} \sum_{\gamma|\gamma\in\phi} Q^{\phi\gamma}_{ij} \quad (2)$$

It is implicitly assumed in the framework that if a bus does not have a connected device (MV transformer, PV, or EVCS), the corresponding active and reactive power related to that device is forced to be zero. In addition, the three-phase active and reactive power balance equations account for the self and mutual impedance of all phases. In (1) and (2), the $P^{\varphi\gamma}_{ij}$ and $Q^{\varphi\gamma}_{ij}$ can be written as:

$$\forall(i,j)\in L,\varphi,\gamma\in\phi$$
$$P_{ij}^{\varphi\gamma}=\frac{\begin{array}{r}R_{ij}^{\varphi\gamma}(V_i^{\varphi})^2-R_{ij}^{\varphi\gamma}V_i^{\varphi}V_j^{\gamma}\cos(\theta_i^{\varphi}-\theta_j^{\gamma})\\+X_{ij}^{\varphi\gamma}V_i^{\varphi}V_j^{\gamma}\sin(\theta_i^{\varphi}-\theta_j^{\gamma})\end{array}}{\left(R_{ij}^{\varphi\gamma}\right)^2+\left(X_{ij}^{\varphi\gamma}\right)^2} \tag{3}$$

$$\forall(i,j)\in L,\varphi,\gamma\in\phi$$
$$Q_{ij}^{\varphi\gamma}=\frac{\begin{array}{r}X_{ij}^{\varphi\gamma}(V_i^{\varphi})^2-R_{ij}^{\varphi\gamma}V_i^{\varphi}V_j^{\gamma}\sin(\theta_i^{\varphi}-\theta_j^{\gamma})\\+X_{ij}^{\varphi\gamma}V_i^{\varphi}V_j^{\gamma}\cos(\theta_i^{\varphi}-\theta_j^{\gamma})\end{array}}{\left(R_{ij}^{\varphi\gamma}\right)^2+\left(X_{ij}^{\varphi\gamma}\right)^2} \tag{4}$$

In order to have a convex optimization model and tackle the problem via one of the efficient convex solvers, the linearized forms of (1) and (2) for a single-phase distribution network are taken from [24] and extended to three-phase unbalanced network. Equations (11) and (12) denote branch active and reactive power losses and are defined based on the linearized power flow expression captured in (5)-(10). As justifiable assumptions in distribution networks, it is assumed that the voltage magnitudes are around 1 p.u. and the angle differences of successive nodes are close to zero.

$$P_{ij}^{\varphi\gamma}\approx P_{ij-1}^{\hat{\varphi}\gamma}+P_{ij-2}^{\hat{\varphi}\gamma}=\hat{P}_{ij}^{\varphi\gamma} \tag{5}$$

$$Q_{ij}^{\varphi\gamma}\approx Q_{ij-1}^{\hat{\varphi}\gamma}+Q_{ij-2}^{\hat{\varphi}\gamma}=\hat{Q}_{ij}^{\varphi\gamma} \tag{6}$$

$$P_{ij-1}^{\hat{\varphi}\gamma}=\frac{r_{ij}^{\varphi\gamma}x_{ij}^{\varphi\gamma}}{r_{ij}^{\varphi\gamma 2}+x_{ij}^{\varphi\gamma 2}}.\frac{V_i^{\varphi}-V_j^{\varphi}}{x_{ij}^{\varphi\gamma}}=k_{ij-1}^{\varphi\gamma}.\frac{V_i^{\varphi}-V_j^{\varphi}}{x_{ij}^{\varphi\gamma}} \tag{7}$$

$$P_{ij-2}^{\hat{\varphi}\gamma}=\frac{x_{ij}^{\varphi\gamma 2}}{r_{ij}^{\varphi\gamma 2}+x_{ij}^{\varphi\gamma 2}}.\frac{\theta_i^{\varphi}-\theta_j^{\varphi}}{x_{ij}^{\varphi\gamma}}=k_{ij-2}^{\varphi\gamma}.\frac{\theta_i^{\varphi}-\theta_j^{\varphi}}{x_{ij}^{\varphi\gamma}} \tag{8}$$

$$Q_{ij-1}^{\hat{\varphi}\gamma}=\frac{-r_{ij}^{\varphi\gamma}x_{ij}^{\varphi\gamma}}{r_{ij}^{\varphi\gamma 2}+x_{ij}^{\varphi\gamma 2}}.\frac{\theta_i^{\varphi}-\theta_j^{\varphi}}{x_{ij}^{\varphi\gamma}}=-k_{ij-1}^{\varphi\gamma}.\frac{\theta_i^{\varphi}-\theta_j^{\varphi}}{x_{ij}^{\varphi\gamma}} \tag{9}$$

$$Q_{ij-2}^{\hat{\varphi}\gamma}=\frac{x_{ij}^{\varphi\gamma 2}}{r_{ij}^{\varphi\gamma 2}+x_{ij}^{\varphi\gamma 2}}.\frac{V_i^{\varphi}-V_j^{\varphi}}{x_{ij}^{\varphi\gamma}}=k_{ij-2}^{\varphi\gamma}.\frac{V_i^{\varphi}-V_j^{\varphi}}{x_{ij}^{\varphi\gamma}} \tag{10}$$

As a result, (1) and (2) can be replaced with (11) and (12):

$$\begin{aligned}P_{i_{inject}}^{\varphi}+P_{i_{PV}}^{\varphi}&=P_{i_{ld}}^{\varphi}+P_{i_{EV}}^{\varphi}\\&+\sum_{\ell|(i,j)\in L}\sum_{\gamma|\gamma\in\phi}P_{ij}^{\hat{\varphi}\gamma}\end{aligned} \tag{11}$$

$$\begin{aligned}Q_{i_{inject}}^{\varphi}+Q_{i_{PV}}^{\varphi}&=Q_{i_{ld}}^{\varphi}+Q_{i_{EV}}^{\varphi}\\&+\sum_{\ell|(i,j)\in L}\sum_{\gamma|\gamma\in\phi}Q_{ij}^{\hat{\varphi}\gamma}\end{aligned} \tag{12}$$

B. Capacity constraint

The capacity of distribution lines should guarantee the secure operation of the system. So, it can be written as:

$$\begin{aligned}&\forall(i,j)\in\ell,\forall\varphi,\varphi\in\phi\\&S_{ij}^{\varphi\varphi}=\sqrt{P_{ij}^{\varphi\varphi 2}+Q_{ij}^{\varphi\varphi 2}}\leq S_{ij}^{max}\end{aligned} \tag{13}$$

From the optimization problem parameters and variables perspective, the equation (13) is nonlinear and nonconvex. Therefore, linear approximation using the piecewise linearization method [25] is applied to maintain the linear and convex form of the problem and can be shown as:

$$\begin{aligned}&\forall h,h\in N,h\leq H,\forall(i,j)\in\ell,\forall\varphi,\varphi\in\phi\\&\left(\sin\left(\frac{360^{\circ}h}{H}\right)-\sin\left(\frac{360^{\circ}}{H}(h-1)\right)\right)P_{ij}^{\varphi\varphi}-\\&\left(\cos\left(\frac{360^{\circ}h}{H}\right)-\cos\left(\frac{360^{\circ}}{H}(h-1)\right)\right)Q_{ij}^{\varphi\varphi}\\&\leq S_{ij}^{max}\times\sin\left(\frac{360^{\circ}}{H}\right)\end{aligned} \tag{14}$$

C. Voltage constraints: magnitude, imbalance factor

The hard margin voltage magnitude constraint is implemented as follows:

$$\forall i,\varphi,\ i\in N,\varphi\in\phi,\quad V_{min}\leq V_i^{\varphi}\leq V_{max} \tag{15}$$

In (15), the V_{min} and V_{max} are the voltage magnitude limits determined by the standards. In order to maintain power quality standards in unbalanced systems, the VUF standard is considered [26]. Equation (16) demonstrates the definition of VUF.

$$VUF_i=\frac{|V_i^{-}|}{|V_i^{+}|}\leq VUF_{max} \tag{16}$$

It should be mentioned that the hard margin implementation of highly non-linear VUF constraints is impossible in the convex optimization platform. Therefore the two options could be hard margin linear VUF approximation and soft margin quadratic approximation in weighted-sum multiple objective optimization models. It is later discussed in IV-A that the latter is a more accurate approach and is used as a VUF constraint basis in the presented formulation. The quadratic approximation of VUF can be shown as:

$$VUF_i\approx VUF_i^{apr} \tag{17}$$

where:

$$\begin{aligned}VUF_i^{apr}=&\sum_{0\leq n\leq 2}\sum_{0\leq m\leq<n}\sum_{\varphi,\gamma\in\phi}(\alpha_{i_{mn}}^{\varphi\gamma}(V_i^{\varphi})^m(V_i^{\gamma})^{n-m}\\&+\beta_{i_{mn}}^{\varphi\gamma}(V_i^{\varphi})^m(\theta_i^{\gamma})^{n-m}+\delta_{i_{mn}}^{\varphi\gamma}(\theta_i^{\varphi})^m(\theta_i^{\gamma})^{n-m})\end{aligned} \tag{18}$$

D. Objective function

Without loss of generality, the minimum operational cost of the system is sought here as (19).

$$OF \in R,$$
$$OF = \sum_{s\in S}(c_1^s + c_2^s P_{inject_s^\varphi} + c_3^s (P_{inject_s^\varphi})^2) \tag{19}$$

The active power injection of PVs and reactive power support of EVCSs are assumed to be costless. The objective functions can be readily tailored for meshed and multiple input distribution networks connected to MV systems with different cost terms. The objective function can also imply either minimization of the cost or maximization of firm benefit in the highly PV penetrated and reverse power flow enabled systems. It is pretty straightforward to replace it with maximum social welfare, maximum firm benefit, etc., or even proceed with multiple objectives. For this paper, the multi-objective objective function is presented as (20).

$$\begin{aligned} 0 \le w', w_i \le 1,\ OF \in R,\\ OF = w' \sum_{s\in S}(c_1^s + c_2^s P_{inject_s^\varphi} + c_3^s (P_{inject_s^\varphi})^2)\\ + \sum_{i\in N} w_i VUF_i^{apr} \end{aligned} \tag{20}$$

The weight coefficient w_i is flexible to be customized for each bus to prioritize the power quality constrain in certain buses. In other words, it improves the imbalance of a particular bus by exploiting the existing system flexibility in the operation without performing local modifications or installations. The weight coefficients used in the current approach are further discussed in IV-B.

E. EVCS models

EVCSs are considered both single- and three-phase in the distribution systems. While they can flexibly provide reactive power based on system optimization, their consumed active power is assumed to be constant and adjusted based on the customer charging preference and the battery and inverter capability in a certain period. Nevertheless, they can provide flexibility over consumed active power in each time interval thanks to their schedulability. Because we are targeted to perform the optimization in the near real-time scope to handle random phenomena, we prefer to ignore this capability, at least in the scope of this study. The formulation of a single-phase EVCS in phase κ is shown in (21)-(23). For simplification, EVCSs are shortened to EVs in the optimization formulations.

$$\forall i, i \in N \quad P_{i_{EV}}^\kappa = P_{i_{EV}}^{sch} \tag{21}$$

$$\forall i, i \in N \ \ \forall \varphi, \varphi \in \phi |\ \varphi \ne \kappa, \quad P_i^{EV} = 0 \tag{22}$$

$$\begin{aligned} \forall i, i \in N \quad -\sqrt{(S_{i_{EV}}^{inv})^2 - (P_{i_{EV}}^\kappa)^2} \le Q_{i_{EV}}^\kappa\\ \le +\sqrt{(S_{i_{EV}}^{inv})^2 - (P_{i_{EV}}^\kappa)^2} \end{aligned} \tag{23}$$

The variable $Q_{i_{EV}}^\kappa$ can be derived based on the result of the optimization problem. Equations (24)-(26) show the three-phase EVCS model and corresponding linearization. In the three-phase case, (21) and (22) are changed to (24), in which the cross-phase active power transfer is also enabled.

$$\forall i \in N, \sum_{\varphi\in\phi} P_{i_{EV}}^\varphi = P_{i_{EV}}^{sch} \tag{24}$$

$$\forall i, i \in N, \forall \varphi, \varphi \in \phi, \quad \sqrt{(P_{i_{EV}}^\varphi)^2 + (Q_{i_{EV}}^\varphi)^2} \le S_{i_{EV}}^{inv} \tag{25}$$

$$\begin{aligned} \forall h, h \in H, \forall i, i \in N, \forall \varphi, \varphi \in \phi\\ \left(\sin\left(\frac{360^\circ h}{H}\right) - \sin\left(\frac{360^\circ}{H}(h-1)\right)\right) P_{i_{EV}}^\varphi\\ - \left(\cos\left(\frac{360^\circ h}{H}\right) - \cos\left(\frac{360^\circ}{H}(h-1)\right)\right) Q_{i_{EV}}^\varphi\\ \le S_{i_{EV}}^{inv} \times \sin\left(\frac{360^\circ}{H}\right) \end{aligned} \tag{26}$$

Therefore, corresponding $P_{i_{EV}}^\varphi$(cross-phase active power) can be derived based on the optimization results as well as the $Q_{i_{EV}}^\varphi$. The noteworthy point is that even during the off hours of EVCSs, the active power can be transferred between phases like an active power line conditioner [14]. This capability enables the EVCSs to provide more active ancillary services if needed and makes them more economically reasonable.

F. PVs model

Like the EVCSs, PVs are installed as three-phase and single-phase in distribution networks. While the three-phase PVs can contribute to the balancing and voltage magnitude control, the single-phase configurations may harm the system's power quality when used uncontrolled. Therefore, PV management not only can help the optimization problem to have enough flexibility to satisfy its objective, but also it is necessary for maintaining the power quality standards. The single-phase PV in phase κ can be modeled as:

$$\forall i, i \in N,\ 0 \le P_{i_{PV}}^\kappa \le P_{i_{PV}}^{sun} \tag{27}$$

$$\forall i, i \in N,\ \forall \varphi, \varphi \in \phi | \varphi \ne \kappa,\ P_{i_{PV}}^\varphi = 0 \tag{28}$$

$$\forall i, i \in N,\ \sqrt{\left(P_{i_{PV}}^\kappa\right)^2 + \left(Q_{i_{PV}}^\kappa\right)^2} \le S_{i_{PV}}^{inv} \tag{29}$$

With the linear approximation, (29) can be replaced by:

$$\begin{aligned} \forall h, h \in H, \forall i, i \in N,\\ \left(\sin\left(\frac{360^\circ h}{H}\right) - \sin\left(\frac{360^\circ}{H}(h-1)\right)\right) P_{i_{PV}}^\kappa\\ - \left(\cos\left(\frac{360^\circ h}{H}\right) - \cos\left(\frac{360^\circ}{H}(h-1)\right)\right) Q_{i_{PV}}^\kappa\\ \le S_{i_{PV}}^{inv} \times \sin\left(\frac{360^\circ}{H}\right) \end{aligned} \tag{30}$$

The corresponding $P^{\kappa}_{i_{PV}}$ and $Q^{\kappa}_{i_{PV}}$ are derived from the optimization problem. The three-phase PV model and the approximation are presented in (31),(32), and (33), respectively:

$$\forall i \in N,\ 0 \leq \sum_{\varphi \in \phi} P^{\varphi}_{i_{PV}} \leq P^{sun}_{i_{PV}} \tag{31}$$

$$\forall i, i \in N, \forall \varphi, \varphi \in \phi, \quad \sqrt{(P^{\varphi}_{i_{PV}})^2 + (Q^{\varphi}_{i_{PV}})^2} \leq S^{inv}_{i_{PV}} \tag{32}$$

$$\begin{aligned} &\forall h, h \in H, \forall i, i \in N, \forall \varphi, \varphi \in \phi \\ &\left(\sin\left(\frac{360^\circ h}{H}\right) - \sin\left(\frac{360^\circ}{H}(h-1)\right)\right) P^{\varphi}_{i_{PV}} \\ &- \left(\cos\left(\frac{360^\circ h}{H}\right) - \cos\left(\frac{360^\circ}{H}(h-1)\right)\right) Q^{\varphi}_{i_{PV}} \\ &\leq S^{inv}_{i_{PV}} \times \sin\left(\frac{360^\circ}{H}\right) \end{aligned} \tag{33}$$

Finally, the $P^{\varphi}_{i_{PV}}$ and $Q^{\varphi}_{i_{PV}}$ can be derived fromfrom the optimization problem. To sum up, the QP framework will be the minimization of the objective function of (19) subject to (11), (12), (14), (23)-(27), (29)-(31), (33), (34) and (36).

III. Computational Implementation

A. Input Structure and Test Cases

The input Data structure is built and developed based on the MATPOWER structure [27]. The Matpower test case structure is modified from single-line balanced to three-phase unbalanced in order to be able to add the three-phase unbalanced test cases to the case library. For this paper, two unbalanced standard systems are added to the Matpower library; the IEEE 33 Bus [28] and the 192 LV buses of the IEEE 342-bus test system [29]. The two systems are chosen to cover different voltage levels, bus numbers, topology types (meshed or radial), and several slack buses. The IEEE 33-bus system is modified to be a balanced three-phase system, and then the loads are forced to be unbalanced by the load intensity factor, which will be defined later in the paper. However, the 192 LV buses of the IEEE 342-bus test system are inherently unbalanced, heavily meshed, and connected to the MV system from different nodes to maintain reliability and satisfy the high load density. Single-phase and three-phase PV and EVCs with different penetration levels are added to the test cases for this research. Fig. 1 demonstrates the PV and EV locations of the mentioned systems, respectively. It is worth mentioning that the location of EVs and PVs are occasionally overlapped to create a more intense test environment for the proposed method. The details of the test system parameters are elaborated using the table I.

B. Method Clustering

The proposed method is clustered into Five sub-methods presented in table II to form an ablation study. The *Fixed* method is a regular OPF solver in Matpower extended to three-phase systems. Consequently, three-phase EVs and PVs have been considered three single-phase models. The *OPF* method is the linearized form of the *Fixed* method solved in CVX.

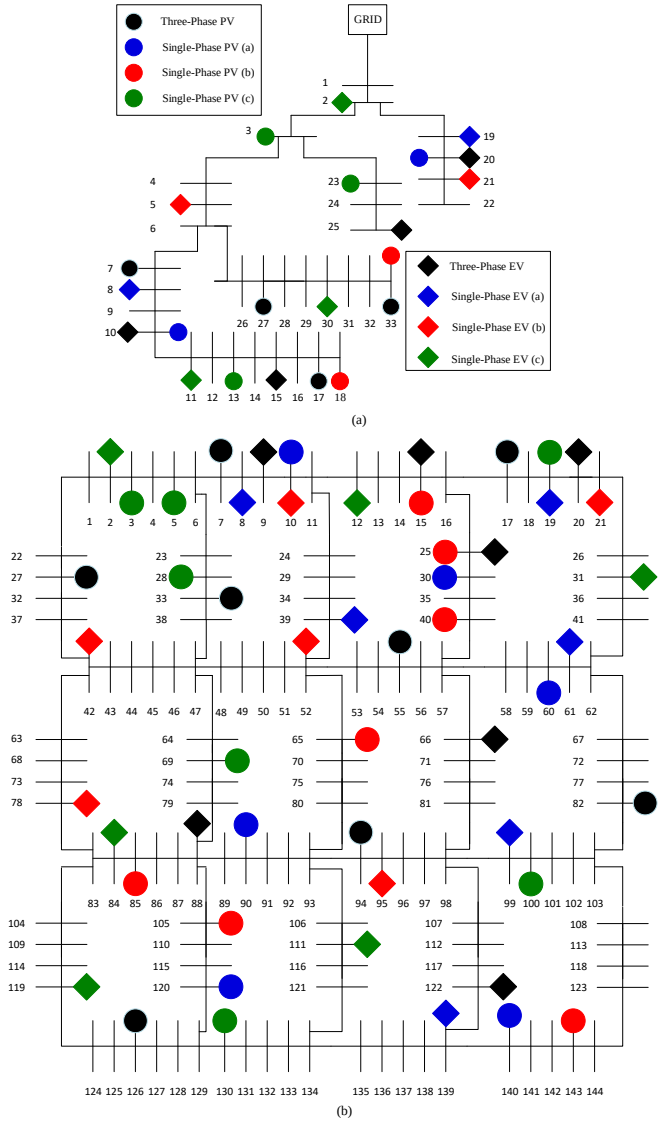

Fig. 1. a) IEEE 33-bus, b) 192-bus system

TABLE I
System Parameters

System	33-Bus	192-Bus
L-n Voltage	12.6kv	120
Min Voltage	0.9 p.u	0.9 p.u
Max Voltage	1.1 p.u	1.1 p.u
Cost Coefficient c_1	3	3
Cost Coefficient c_2	0.1	0.1
Cost Coefficient c_3	0	0
Base MVA	100MVA	100MVA
Sum of Loads	3.75MW	2.9MW
Average of Loads	0.11MW	0.02MW
Sum of Reactive Loads	2.3MW	1.82MW
Average of Reactive Loads	0.07MVAR	0.012MVAR
Three-phase EV Capacity	0.54MVA	0.12MVA
Three-phase EV Active Power Consumption	0.18MVA	0.06MVA
Three-phase PV Capacity	0.9MVA	0.3MVA
Three-phase PV Ative Power Generation	0.54MVA	0.15MVA
Slack Bus Locations	1	144-192

TABLE II
SUB-METHODS USED FOR ABLATION STUDY

Sub-Method	Solver	Equations
Fixed	Matpower	(1-4), (13), (15), (19), (21), (23), (27), (29)
OPF	CVX	(5-12), (14-15), (19), (21), (23), (27), (30)
OPF VUF	CVX	(5-12), (14-15), (18), (20-21), (23), (27), (30)
Crossphase	CVX	(5-12), (14-15), (19), (21-22), (23-24), (26-28), (30-31), (33)
Crossphase VUF	CVX	(5-12), (14-15), (18), (20-22), (23-24), (26-28), (30-31), (33)

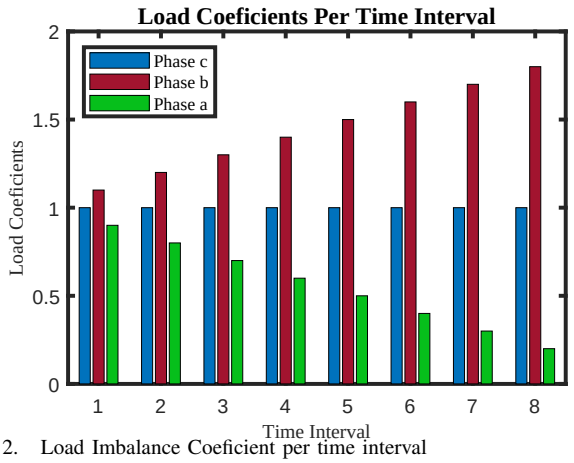

Fig. 2. Load Imbalance Coeficient per time interval

The *OPF VUF* method is the *OPF* method that considers the VUF constraint. Similarly, the *Cross-Phase* method is the *OPF*, enabling the Cross-Phase capability of PVs and EVs. Finally, the *Cross-Phase VUF* method integrates all the contributions of this paper into one method. Both Matpower and CVX solvers are run in the MATLAB 2022a, Intel Core i5 8250U (1.6-1.8 GHz) CPU, and 8 GB DDR3-1333 (667 MHz) memory Environment.

C. Operation Scenarios and time intervals

In order to test the individual and combined contribution of each inverter type, four scenarios are considered. These scenarios are named *Base(NC)*, *PV-noon(NC)*, *Ev-night(NC)*, and *PV-EV-Afternoon*. In addition, unlike the *Fixed*, *OPF*, and *OPF-VUF* methods, *Cross-Phase* and *Cross-Phase OPF* methods can exploit the active power capacity of the inverters in their non-operation hours. In other words, non-operation hours for PVs and EVS are night and day, respectively. Accordingly, three more scenarios are added to elevate the contribution of each inverter type in non-operational hours. These scenarios are *Base(C)*, *PV-noon(C)*, and *Ev-night(C)*. So, the proposed method can use the capacity of the inverters during non-operational hours.

All of the scenarios consist of eight intervals, each having a different load imbalance level, as shown in Fig. 2. The load imbalance (Active and Reactive) is getting worse linearly in each interval while maintaining a constant total load consumption in order to obtain standardized load flow results.

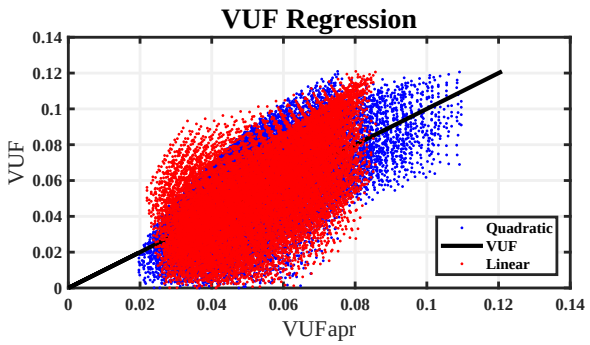

Fig. 3. Scatter Plot of Linear and Quadratic Regression of VUF

IV. PARAMETER TUNING

A. VUF Quadratic Regression

In (18), the $\alpha_{imn}^{\varphi\gamma}$ $\beta_{imn}^{\varphi\gamma}$ $\delta_{imn}^{\varphi\gamma}$ can be approximated by a data-driven regression method trained on VUF results of large data points of voltage angle and magnitude in the operational range. For this study, the data points are created by sweeping voltage magnitude from $V_{min} = 0.9$ to $V_{max} = 1.1$ with 0.1 increments, and angles are swept between -5° to 5° with 1° increments. The leveraged data-driven method is the least square multi-variable quadratic regression. Figure represents the scatter plot of both linear and quadratic regressions. As it can be shown in the figure the although the quadratic regression has a large approximation error due to the high non-linearity of VUF function, it is relatively better that the linear results. Therefore the weighted-sum multiple objective approach is more accurate than hard margin linear VUF implementation. The resultant parameters are embedded to the *OPF VUF* and *Crossphase VUF* methods.

B. Pareto Front Trade-Off

In order to enable a quantified trade-off between cost and the sum of VUFs, the Pareto method is used. For having a 2D Pareto Front, it is assumed that all buses have the same weight and $w' = (1-w)$. The Pareto front with 0.1 increments for the *Crossphase VUF* method is illustrated in figure 4 for the *PVEV afternoon* scenario. it can be seen that there is a significant reduction in the sum for all time intervals of VUFs when increasing w from 0 to 0.1. However, a further increase of w seems not to significantly decrease the VUF sum value while it increases the cost drastically. Therefore, the $w = 0.1$ is used in the proposed weighted sum method.

V. RESULTS AND DISCUSSION

This section compares the effectiveness of the presented sub-methods and scenarios in four aspects; 1) total cost, 2) voltage imbalance, 3) total loss, and 4) line capacity utilization. For each of the mentioned aspects, first, the II sub-methods are compared in the complete scenario, *PVEV afternoon*. Then the III-C scenarios are compared for the state-of-the-art method, *CrossPhase VUF*.

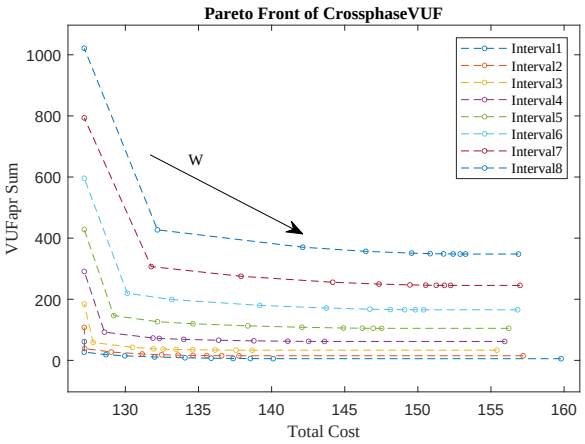

Fig. 4. Pareto front of *Crossphase VUF* method in *PVEV afternoon* scenario

TABLE III
TOTAL COST OF THE IEEE SYSTEMS DURING " PV-EV-AFTERNOON" SCENARIO DURING 5TH TIME INTERVAL

System	Fixed	OPF	OPF-VUF	Crossphase	Crossphase-VUF
33-Bus	346.54	346.54	351.72	341.29	344.55
192-Bus	127.19	127.19	147.22	127.19	142.07

TABLE IV
TOTAL COST OF THE IEEE 33- AND 192-BUS SYSTEMS WHILE IMPLEMENTING CROSSPHASE VUF FOR DIFFERENT SCENARIOS DURING 5TH TIME INTERVAL

Scenarios	Base (C)	Base (NC)	EV-Night(C)	EV-Night(NC)	PV-Noon(C)	PV-Noon(NC)
33-Bus	361.87	367.81	369.94	373.40	337.35	339.27
192-Bus	155.19	155.19	171.19	171.19	126.94	129.92

A. Total cost of the studied systems

The total cost of the systems for the sub-methods of Table. II is evaluated for the fifth time interval in Table.III. Assessing the Table proves that using a cross-phase enabled sub-method reduces the total cost of the systems in both test systems. As it is visible, utilizing the other sub-methods is less profitable than the cross-phase. This cost reduction is achieved by exploiting the capacity of PV and EV inverters during operational and non-operational hours in *Crossphase* and *Crossphase VUF* methods. Fig. 5 compares the apparent, active, and reactive power reference of the three-phase EV charger installed on bus number 88 of the IEEE 192 bus system for both *Crossphase* and *OPF* methods during operational and non-operational hours. The figure shows that the inverter capacity utilization in operational mode is 5% more when Cross-Phase is enabled. Moreover, in non-operational hours, Cross-Phase enables the inverter to circulate the active power by consuming power from phase c and transferring it to phase b to compensate for the induced load imbalance shown in figure 2. Also, as shown in Table. IV, the total cost of the *Cross-Phase VUF* is lesser in the scenarios that enable the inverters to contribute in non-operational hours than in the scenarios that turn the inverters off during non-operation. This resultant Cross-Phase flexibility leads to a better optimal solution in terms of cost. Due to the meshed topology of the IEEE 192 bus, enabling Cross-Phase is not guaranteed as in the IEEE 33 bus radial system. This behavior is related to possible current imbalance propagation to several main lines in meshed grids, further discussed in V-C. Another result can be obtained from the Table. IV is that although both systems have more PVs in capacity and numbers installed, EVs show a better non-operational Cross-Phase contribution to cost reduction.

Sub-methods that contain a VUF constraint experience a higher total cost because of the additional term in their objective functions. In both systems, intensifying the load imbalance will increase system cost in VUF-constrained sub-methods. The cost difference between the VUF-constrained and nonconstrained sub-methods is the price that should be paid for compensation of the VUF.

B. Voltage Imbalance

Figures 6 and 7 compare the results of the VUF for each bus in all time intervals with the mentioned sub-methods of the table. II. The results show the superiority of *Cross-Phase VUF* in reducing the VUF compared to others. Also, the VUF *Cross-Phase* reduces VUF; however, the effect of VUF constraint is more than Cross-Phase individually. The VUF *OPF* and *Fixed* method are only different in their linearity of constraints, and the solver shows a very severe VUF, especially in intense time intervals.

The results for the Scenarios other than *PVEV afternoon* are summarized in the Table. V. This table shows only the results for the most extreme condition (time interval 8). According to the table, however, the standard could not be maintained in this worst-case scenario; the Cross-Phase contribution of EVs and PVs significantly reduced the nonstandard-conditioned buses. Also, results reveal that, unlike the cost, in terms of VUF reduction, the Cross-Phase contribution of PVs in both *Base (C)* and *EV Night (C)* are more effective than the Cross-Phase contribution of EVs such in IEEE 33 bus systems they were able to reach a standard solution. The results also reveal that

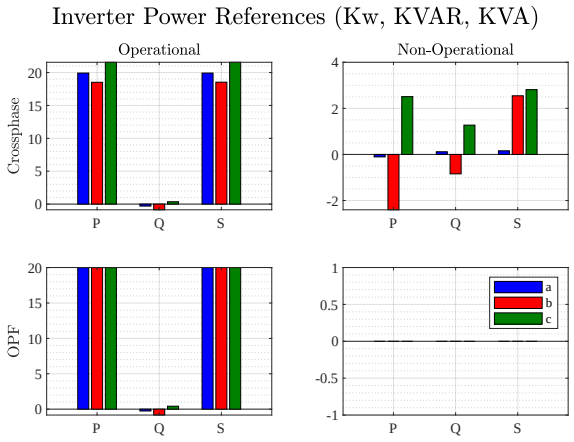

Fig. 5. Comparison Between *Crossphase* and *OPF* Methods in Exploiting the Apparent Power Capacity in a Three-Phase Inverter (EV in bus 89 of 192 bus test system) During Operational and Non-Operational Modes

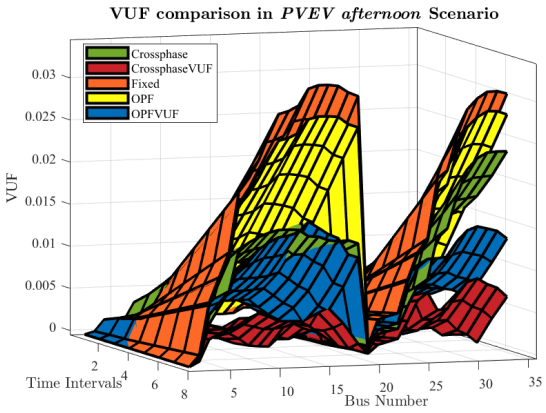

Fig. 6. VUF Comparison of sub-methods in *PVEV afternoon* scenario in 33 bus system

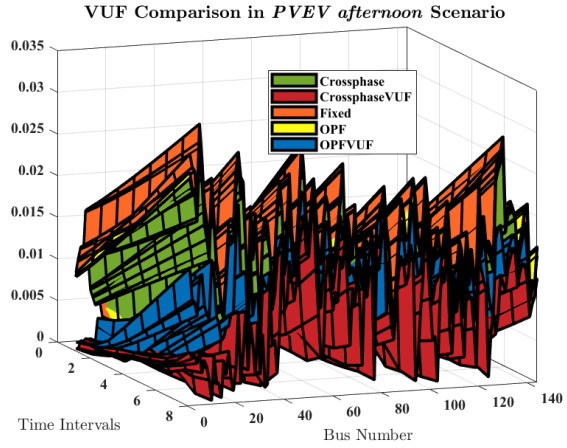

Fig. 7. VUF Comparison of sub-methods in *PVEV afternoon* scenario in 192 bus system (Slack buses are not shown)

the Cross-Phase capability is more effective in radial 33 bus than the heavily meshed 192 bus system.

C. Total power loss of the test systems

The total power loss of the test systems for different sub-methods is pointed out in Tables. VI and VII. Analyzing Table.VI clears that by increasing load imbalance intensity, total power loss of the IEEE 33-Bus system experiences an upward trend. Due to the constant three-phase load power in all intervals, it can be concluded that the increase in loss is solely a result of the increase in the line imbalance. Before discussing the relation between line imbalance and Cross-Phase, it must be mentioned that the Cross-Phase operation for the cost and VUF minimization can have two forms: 1) allocating power of the inverter to meet the unbalanced load demand. 2) transferring flowing power from a collection of single-phase PVs in one phase to another. The first form will locally compensate for the line imbalance of the lower side and can have a balancing effect on the upper main line in radial systems. The latter, however, will exploit the line capacity to transfer a generated single-phase power to the upper side loads or loads in the other phases and may not guarantee a balanced upper main line. Considering the above mentioned, it can be seen that on the Table. VI, when the loads are nearly balanced (intervals 1-3), *Cross-Phase VUF* compromises the line imbalance and the loss to reach a better VUF and cost. However, in highly unbalanced situations, the *Cross-Phase VUF* minimizes the VUF and cost without compromising the loss. Therefore, current and voltage imbalance are minimized alongside the cost in these cases. Analyzing the results of the Table. VII reveals that in the presented heavily meshed grid, the loss in *Cross-Phase VUF* is more than *Cross-Phase* in all time intervals, which means that the line imbalance must be compromised to reach a better VUF. This behavior is like the behavior of the radial grid between (1-3) intervals. Therefore it can be concluded that the voltage and current imbalance are not always inlined.

The scenario-based results are presented in tables VIII and IX. According to 33 Bus system results, the non-operational contribution of EVs and PVs both worked in favor of the system loss reduction in all intervals, which illustrates the superiority of Cross-Phasing in radial topology in terms of loss. In analyzing, different conclusions can be made. First, comparing the results of *Base (NC)* and *(C)* for interval one where there is no single-phase generation reveals that attempt to reduce VUF and cost will propagate line imbalance due to meshed topology. This result shows that the claim made for the first Cross-Phasing form is not valid in meshed networks. Second, in comparing the results of *EV Night (NC)* and *(C)*, where the cross phasing is dined by PVs, and a lot of single-phase generation exists, loss reduction will not occur before interval 7, which supports the claim made in the previous paragraph about the second form of cross-phasing. On the other hand, *PV noon (NC)* and *(C)* show that only EV cross-phasing in the entire presence of PVs could successfully reduce the loss in all time intervals.

TABLE V
PERCENTAGE OF THE BUSES OF IEEE 33 AND 192-BUS SYSTEM VIOLATING THE IEEE 1159 STANDARD DURING DIFFERENT SCENARIOS (%)

Test system	Base (NC)	Base (C)	PV-Noon (NC)	PV-Noon (C)	EV-Night (NC)	EV-Night (C)
33-Bus	76	0	24	6	69	0
342-Bus	75	43	46	41	71	44

VI. CONCLUSION

This paper introduced a convex, nearly exact AC three-phase optimal power flow applicable in both meshed and radial networks to optimally manage the per-phase active and reactive power references of single and three-phase PVs and EVs in an active distribution network. The method is tested on two test cases and four operational scenarios, including incremental sub-methods that lead to the proposed state-of-the-art method. Each contribution and their reflection on the results

TABLE VI
TOTAL POWER LOSS IN IEEE 33-BUS SYSTEM WITH DIFFERENT DISPATCHING METHODS (KW)

Hour	Fixed	OPF	OPF-VUF	Crossphase	Crossphase-VUF
1	4.88	4.87	4.68	4.86	5.01
2	4.98	4.97	4.81	4.92	5.05
3	5.15	5.14	5.13	5.06	5.16
4	5.39	5.37	5.35	5.26	5.32
5	5.70	5.69	5.60	5.54	5.56
6	6.08	6.07	5.91	5.88	5.86
7	6.53	6.52	6.29	6.29	6.22
8	7.06	7.04	6.75	6.78	6.66

TABLE VII
TOTAL POWER LOSS IN IEEE 192-BUS SYSTEM WITH DIFFERENT DISPATCHING METHODS (KW)

Hour	Fixed	OPF	OPF-VUF	Crossphase	CrossPhase-VUF
1	14.15	14.40	15.51	14.42	14.80
2	14.47	14.72	16.11	14.72	14.82
3	15.00	15.25	16.62	15.24	15.14
4	15.74	16.00	17.16	15.95	15.99
5	16.70	16.94	17.85	16.86	17.29
6	17.87	18.07	18.72	17.92	18.53
7	19.25	19.43	19.81	19.29	19.79
8	20.85	21.00	21.09	20.81	20.97

TABLE VIII
TOTAL POWER LOSS OF THE 33-BUS SYSTEM WITH CROSSPHASE-VUF METHOD DURING DIFFERENT SCENARIOS (KW)

Hour	1	2	3	4	5	6	7	8
Base(C)	5.22	5.20	5.09	5.37	5.69	5.83	5.98	6.11
Base (NC)	5.31	5.41	5.59	5.83	6.15	6.53	6.99	7.51
EV-Night (C)	5.87	5.74	5.66	5.78	6.31	6.66	6.49	6.76
EV-Night (NC)	6.27	6.06	6.03	6.17	6.38	6.66	7.01	7.40
PV-Noon (C)	2.43	2.68	3.12	3.35	3.32	3.07	3.89	4.48
PV-Noon (NC)	2.80	2.79	2.85	2.96	3.23	3.67	4.46	5.06

TABLE IX
TOTAL POWER LOSS OF THE 192-BUS SYSTEM WITH CROSSPHASE-VUF METHOD IN DIFFERENT SCENARIOS (KW)

Hour	1	2	3	4	5	6	7	8
Base(C)	16.72	16.85	17.17	17.79	18.53	19.35	20.31	21.38
Base (NC)	16.48	16.79	17.32	18.06	19.00	20.16	21.53	23.11
EV-Night (C)	19.85	20.02	20.38	21.01	21.77	22.64	23.57	24.69
EV-Night (NC)	19.60	19.77	20.17	20.79	21.59	22.58	23.77	25.18
PV-Noon (C)	12.52	12.70	12.98	13.64	14.93	16.12	17.30	18.46
PV-Noon (NC)	12.68	12.87	13.32	14.24	15.68	16.97	18.40	19.77

are concluded as follows: 1) The explicit consideration of voltage angle and magnitude enabled the method to include the VUF as an operational objective such that the results showed significant regulation of VUFs while using this optimization method. Sub-methods containing a VUF constraint experience a higher total cost because of the additional term in their objective functions while showing superiority in reducing the VUF. Therefore, the cost difference between the VUF-constrained and non-constrained sub-methods is the price that should be paid for compensation of the VUF .2) VUF constrained is excluded as a constraint and implemented as a secondary objective function with a quadratic multi-variable polynomial approximation over an inclusive data set in the operational range of voltage magnitudes and angles. The rest of the constraints, including power flow and capacity equations, are linearized before implementation. These considerations guarantee a decent computational performance thanks to a quadratic formulation of the optimization problem that can be solved by fast convex solvers. The results of the Sedumi solver showed a decent run time even in the 118 bus system. 3) A Pareto front trade-off has been made to obtain a favorable trade-off between VUF and cost. Results of the Pareto front showed that the weight of the VUF term in objective function does not significantly impact the overall VUF reduction. In other words, the two objectives are not significantly compromising each other, and multi-objective optimization is an excellent approach to reach a desirable VUF and cost simultaneously. 4) The Cross-Phase feature of three-phase EVs and PVs enables the total contribution of the inverter to the optimal operation thanks to the exploitation of their unused capacity. The method comparison results revealed that using cross-phase-enabled sub-methods reduces the total cost. 5) concurrent optimization of EVs and PVs revealed that the EVs show a better non-operational cross-phase contribution to cost reduction. However, the VUF reduction is more contingent on PV optimal operation due to the single-phase PVs. 6) It is also shown in the results that this cross-phase capability can also be beneficial in non-operational modes of PVs and EVs. Results for multiple scenarios showed that enabling non-operational cross-phase leads to a better lower cost and a significantly lower VUF.

REFERENCES

[1] P. Paranavithana, S. Perera, R. Koch, and Z. Emin, "Global voltage unbalance in mv networks due to line asymmetries," *IEEE transactions on power delivery*, vol. 24, no. 4, pp. 2353–2360, 2009.

[2] W. Kong, K. Ma, and Q. Wu, "Three-phase power imbalance decomposition into systematic imbalance and random imbalance," *IEEE Transactions on Power Systems*, vol. 33, no. 3, pp. 3001–3012, 2017.

[3] V. Borozan, D. Rajicic, and R. Ackovski, "Minimum loss reconfiguration of unbalanced distribution networks," *IEEE Transactions on Power Delivery*, vol. 12, no. 1, pp. 435–442, 1997.

[4] A. B. Morton and I. M. Mareels, "An efficient brute-force solution to the network reconfiguration problem," *IEEE Transactions on Power Delivery*, vol. 15, no. 3, pp. 996–1000, 2000.

[5] E. Dall'Anese and G. B. Giannakis, "Sparsity-leveraging reconfiguration of smart distribution systems," *IEEE transactions on power delivery*, vol. 29, no. 3, pp. 1417–1426, 2014.

[6] F. Ding and K. A. Loparo, "Feeder reconfiguration for unbalanced distribution systems with distributed generation: A hierarchical decentralized approach," *IEEE Transactions on Power Systems*, vol. 31, no. 2, pp. 1633–1642, 2015.

[7] Y.-Y. Fu and H.-D. Chiang, "Toward optimal multiperiod network reconfiguration for increasing the hosting capacity of distribution networks," *IEEE Transactions on Power Delivery*, vol. 33, no. 5, pp. 2294–2304, 2018.

[8] J. Zhu, M.-Y. Chow, and F. Zhang, "Phase balancing using mixed-integer programming [distribution feeders]," *IEEE transactions on power systems*, vol. 13, no. 4, pp. 1487–1492, 1998.

[9] T.-H. Chen and J.-T. Cherng, "Optimal phase arrangement of distribution transformers connected to a primary feeder for system unbalance improvement and loss reduction using a genetic algorithm," in *Proceedings of the 21st International Conference on Power Industry Computer Applications. Connecting Utilities. PICA 99. To the Millennium and Beyond (Cat. No. 99CH36351)*. IEEE, 1999, pp. 145–151.

[10] M. W. Siti, D. V. Nicolae, A. A. Jimoh, and A. Ukil, "Reconfiguration and load balancing in the lv and mv distribution networks for optimal performance," *IEEE transactions on power delivery*, vol. 22, no. 4, pp. 2534–2540, 2007.

[11] F. Ding and M. J. Mousavi, "On per-phase topology control and switching in emerging distribution systems," *IEEE Transactions on Power Delivery*, vol. 33, no. 5, pp. 2373–2383, 2018.

[12] G. E. Valderrama, P. Mattavelli, and A. M. Stankovic, "Reactive power and imbalance compensation using statcom with dissipativity-based control," *IEEE Transactions on Control Systems Technology*, vol. 9, no. 5, pp. 718–727, 2001.

[13] R. C. Pires, "Unbalanced phase-to-phase voltage compensators applied to radial distribution feeders," *IEEE transactions on power delivery*, vol. 19, no. 2, pp. 806–812, 2004.

[14] P. Salmerón, J. Montano, J. Vázquez, J. Prieto, and A. Pérez, "Compensation in nonsinusoidal, unbalanced three-phase four-wire systems with active power-line conditioner," *IEEE transactions on power delivery*, vol. 19, no. 4, pp. 1968–1974, 2004.

[15] Y. Xu, J. D. Kueck, L. M. Tolbert, and D. T. Rizy, "Voltage and current unbalance compensation using a parallel active filter," in *2007 IEEE Power Electronics Specialists Conference*. IEEE, 2007, pp. 2919–2925.

[16] M. Singh, V. Khadkikar, A. Chandra, and R. K. Varma, "Grid interconnection of renewable energy sources at the distribution level with power-quality improvement features," *IEEE transactions on power delivery*, vol. 26, no. 1, pp. 307–315, 2010.

[17] S. Weckx and J. Driesen, "Load balancing with ev chargers and pv inverters in unbalanced distribution grids," *IEEE Transactions on Sustainable Energy*, vol. 6, no. 2, pp. 635–643, 2015.

[18] E. Dall'Anese, G. B. Giannakis, and B. F. Wollenberg, "Optimization of unbalanced power distribution networks via semidefinite relaxation," in *2012 North American Power Symposium (NAPS)*. IEEE, 2012, pp. 1–6.

[19] B. A. Robbins and A. D. Domínguez-García, "Optimal reactive power dispatch for voltage regulation in unbalanced distribution systems," *IEEE Transactions on Power Systems*, vol. 31, no. 4, pp. 2903–2913, 2015.

[20] L. R. Araujo, D. Penido, S. Carneiro, and J. L. R. Pereira, "A three-phase optimal power-flow algorithm to mitigate voltage unbalance," *IEEE Transactions on Power Delivery*, vol. 28, no. 4, pp. 2394–2402, 2013.

[21] X. Su, M. A. Masoum, and P. J. Wolfs, "Optimal pv inverter reactive power control and real power curtailment to improve performance of unbalanced four-wire lv distribution networks," *IEEE Transactions on Sustainable Energy*, vol. 5, no. 3, pp. 967–977, 2014.

[22] Q. Nguyen, H. V. Padullaparti, K.-W. Lao, S. Santoso, X. Ke, and N. Samaan, "Exact optimal power dispatch in unbalanced distribution systems with high pv penetration," *IEEE Transactions on Power Systems*, vol. 34, no. 1, pp. 718–728, 2018.

[23] K. Sheshyekani, I. Jendoubi, M. Teymuri, M. Hamzeh, H. Karimi, and M. Bayat, "Participation of distributed resources and responsive loads to voltage unbalance compensation in islanded microgrids," *IET Generation, Transmission & Distribution*, vol. 13, no. 6, pp. 858–867, 2019.

[24] H. Yuan, F. Li, Y. Wei, and J. Zhu, "Novel linearized power flow and linearized opf models for active distribution networks with application in distribution lmp," *IEEE Transactions on Smart Grid*, vol. 9, no. 1, pp. 438–448, 2016.

[25] T. Akbari and M. T. Bina, "Linear approximated formulation of ac optimal power flow using binary discretisation," *IET Generation, Transmission & Distribution*, vol. 10, no. 5, pp. 1117–1123, 2016.

[26] J. Smith, G. Hensley, and L. Ray, "Ieee recommended practice for monitoring electric power quality. revis," 2009.

[27] R. D. Zimmerman, C. E. Murillo-Sánchez, and R. J. Thomas, "Matpower: Steady-state operations, planning, and analysis tools for power systems research and education," *IEEE Transactions on power systems*, vol. 26, no. 1, pp. 12–19, 2010.

[28] M. E. Baran and F. F. Wu, "Network reconfiguration in distribution systems for loss reduction and load balancing," *IEEE Power Engineering Review*, vol. 9, no. 4, pp. 101–102, 1989.

[29] K. Schneider, P. Phanivong, and J.-S. Lacroix, "Ieee 342-node low voltage networked test system," in *2014 IEEE PES general meeting—conference & exposition*. IEEE, 2014, pp. 1–5.